Pentagalloylglucose induces autophagy and caspase-independent programmed deaths in human PC-3 and mouse TRAMP-C2 prostate cancer cells

Hongbo Hu,[1,3] Yubo Chai,[1] Lei Wang,[1] Jinhui Zhang,[1] Hyo Jeong Lee,[1,2] Sung-Hoon Kim,[1,2] and Junxuan Lü[1]

[1]The Hormel Institute, University of Minnesota, Austin, Minnesota; [2]Cancer Preventive Material Development Research Center and Institute, College of Oriental Medicine, Kyunghee University, Seoul, Republic of Korea; and [3]College of Food Science and Nutritional Engineering, China Agricultural University, Beijing, The People's Republic of China

Abstract

Penta-1,2,3,4,6-*O*-galloyl-β-D-glucose (PGG) suppresses the *in vivo* growth of human DU145 and PC-3 prostate cancer xenografts in nude mice, suggesting potential utility as a prostate cancer chemotherapeutic or chemopreventive agent. Our earlier work implicates caspase-mediated apoptosis in DU145 and LNCaP prostate cancer cells as one mechanism for the anticancer activity. We show here that, in the more aggressive PC-3 prostate cancer cell line, PGG induced programmed cell deaths lacking the typical caspase-mediated apoptotic morphology and biochemical changes. In contrast, PGG induced patent features of autophagy, including formation of autophagosomes and lipid modification of light chain 3 after 48 hours of PGG exposure. The "autophagic" responses were also observed in the murine TRAMP-C2 cells. Caspase inhibition exacerbated PGG-induced overall death. As for molecular changes, we observed a rapid inhibition of the phosphorylation of mammalian target of rapamycin–downstream targets S6K and 4EBP1 by PGG in PC-3 and TRAMP-C2 cells but not that of mammalian target of rapamycin itself, along with increased AKT phosphorylation. Whereas the inhibition of phosphatidylinositol 3-kinase increased PGG-induced apoptosis and autophagy, experiments with pharmacologic inducer or inhibitor of autophagy or by knocking down autophagy mediator Beclin-1 showed that autophagy provided survival signaling that suppressed caspase-mediated apoptosis. Knocking down of death receptor-interacting protein 1 kinase increased overall death without changing light chain 3-II or caspase activation, thus not supporting death receptor-interacting protein 1–necroptosis for PGG-induction of autophagy or other programmed cell death. Furthermore, PGG-treated PC-3 cells lost clonogenic ability. The induction by PGG of caspase-independent programmed cell death in aggressive prostate cancer cell lines supports testing its merit as a potential drug candidate for therapy of caspase-resistant recurrent prostate cancer. [Mol Cancer Ther 2009;8(10):2833–43]

Introduction

Caspase-mediated apoptosis is commonly induced by cancer chemotherapeutic drugs or ionization radiation therapy. A major challenge for effective therapy stems from the fact that cancer cells evolve and acquire resistance to drug-induced apoptosis over time. Therefore, agents that can induce alternative types of programmed cell death may help to subvert apoptosis-resistant cancer cells for improved therapeutic efficacy. The existence of alternative backup cell death programs for caspase-mediated apoptosis has been well established (1–3). Three main types of programmed cell death have been traditionally classified morphologically/biochemically (1–3): nuclear or apoptotic (caspase mediated or caspase independent); cell death with "autophagic" features without the involvement of chromatin condensation; and necrosis (necroptosis, paraptosis).

Autophagy (self-eating) is an evolutionarily conserved, dynamic, and lysosome-mediated process that begins with the formation of double or multilayer membranous structures (1, 3, 4). Classic autophagy is induced by poor nutrient conditions as a survival response by recycling cytoplasmic components, including organelles, such as reactive oxygen species–damaged mitochondria and endoplasmic reticulum to maintain ATP level. However, when this process occurs in excess, autophagy itself becomes cytotoxic and eventually leads to autophagic cell death. Necrotic cell death represents a rapid cellular response involving mitochondrial reactive oxygen species production, decreased ATP concentration, and other cellular insults. The broad-spectrum caspase inhibitor zVAD-fmk modulates the three major types

Received 4/10/09; revised 8/7/09; accepted 8/10/09; published 10/12/09.

Grant support: The Hormel Foundation, NIH grant CA136953, the Korea Ministry of Education, Science and Technology Medical Research Center grant 2009-0063466.

The costs of publication of this article were defrayed in part by the payment of page charges. This article must therefore be hereby marked *advertisement* in accordance with 18 U.S.C. Section 1734 solely to indicate this fact.

Note: Supplementary material for this article is available at Molecular Cancer Therapeutics Online (http://mct.aacrjournals.org/).

Requests for reprints: Junxuan Lü, Hormel Institute, University of Minnesota, 801 16th Avenue NE, Austin, MN 55912. Phone: 507-437-9680; Fax: 507-437-9606. E-mail: jlu@hi.umn.edu and Sung-Hoon Kim, Cancer Preventive Material Development Research Center and Institute, College of Oriental Medicine, Kyunghee University, 1 Hoegi-dong, Dongdaemun-gu, Seoul 131-701, Republic of Korea. Phone: 82-2-961-9233; Fax: 82-2-964-1074. E-mail: sungkim7@khu.ac.kr

doi:10.1158/1535-7163.MCT-09-0288

of cell death in select model systems: it blocks apoptotic cell death, enhances autophagy, and sensitizes cells to necrotic cell death.

We have shown that penta-1,2,3,4,6-*O*-galloyl-β-D-glucose (PGG), present abundantly in some Oriental medicinal herbs, suppressed the *in vivo* growth of human DU145 prostate cancer xenografts in nude mice at a tested daily dose of 20 mg/kg body weight (5). After the submission of the current manuscript, Kuo et al. (6) have shown a positive inhibitory efficacy of PGG against the growth of the more aggressive human prostate cancer PC-3 cells inoculated into the tibia in nude mice, simulating metastatic growth. These studies support the potential usefulness of PGG as a chemotherapeutic or chemopreventive agent for prostate cancer. In our earlier publication, we documented that PGG induced predominantly caspase-mediated apoptosis in DU145 and LNCaP prostate cancer cells (5). The apoptosis effects were strongly linked to phospho-signal transducers and activators of transcription 3 (STAT3) inactivation in the p53-mutant and AKT-low (PTEN wild type) DU145 cells and reactive oxygen species–driven p53 activation in the p53-wild type, AKT-moderate LNCaP cells, respectively (5). To provide mechanistic insights into the cellular processes and molecular targets of prostate cancer that allow for individualized treatment by PGG, we examined additional prostate cancer cell line models for their cell death responses. The visible cellular responses in PC-3 prostate cancer cell line (null-p53, null-PTEN/high-AKT, null–STAT3; refs. 7, 8) suggested features of autophagy, including prominent cytoplasmic vacuolation under light microscopy after 48 h of PGG exposure while lacking the typical apoptotic morphologies such as cell rounding and detaching. This raised the hypothesis that PGG might induce in PC-3 and other prostate cancer cells autophagy and nonapoptotic programmed cell death.

In the present work, we sought to characterize the nature of the cell deaths induced by PGG and the relationship with AKT–mammalian target of rapamycin (mTOR) signaling cascades, especially the role of autophagy in the prostate cancer cells, focusing on PC-3 model. During autophagy, organelles are engulfed by the membranous vacuoles, often called autophagosomes, which fuse with lysosomes, where the contents are degraded by the lysosomal proteases (3, 4). At the early stage of autophagy, a conjugation system involving *Atg7* and *Atg3* gene products is responsible for the addition of a phosphatidylethanolamine moiety to the microtubule-associated protein 1 light chain 3 (LC3; *Atg8* gene product), promoting its translocation to membrane vesicles that form the autophagosomes. These subcellular features can be visualized by microscopy as perinuclear punctuate patterns. The lipid modification of LC3 results in a 2-kD decrease in its apparent size on SDS-gel electrophoresis and can be conveniently detected by Western blot (1). Autophagy is mediated by type III phosphatidylinositol 3-kinase complex containing the *Atg6* gene product Beclin-1 (9). Type III phosphatidylinositol 3-kinase is the putative target of 3-methyladenine, which is often used as an inhibitor of autophagy. Beclin-1 is a Bcl-2–interacting protein, and its autophagy function is interrupted by binding to Bcl-2/xL (9). Activation of the mTOR pathway is involved in the suppression of autophagy, and conversely, mTOR inhibition induces autophagy in many models (10). The death receptor-interacting protein 1 (RIP1) kinase is involved in regulating necroptosis and autophagic cell death (2, 3). Therefore, we used pharmacologic inhibitors, as well as siRNA knockdown, to interrogate the relationships of autophagy response with caspase-mediated apoptosis and other types of cell deaths induced by PGG in PC-3 and other prostate cancer cells.

Materials and Methods

Chemicals and Reagents

PGG was isolated from the gallnut of *Rhus chinensis* (11). The purity was ~98%. The general caspase inhibitor (zVADfmk) was purchased from MP-Biomedicals, Inc. Antibodies specific for cleaved poly(ADP-ribose) polymerase (PARP; p89), caspase-8, cleaved caspase-3, and caspase-9 were purchased from Cell Signaling Technology. Antibody for LC3 was purchased from MBL International, Inc. Antibodies for Beclin-1 and death RIP1 were from purchased from Santa Cruz Biotechnologies.

Cell Culture and Treatments

The DU145 and PC-3 cell lines were purchased from the American Type Culture Collection. They were grown under American Type Culture Collection recommended culture medium and 5% CO_2 conditions at 37°C in humidified incubators. Briefly, PC-3 cells were grown in F-12K medium with 10% fetal bovine serum without antibiotics. DU145 cells were grown in minimal essential medium supplemented with 10% fetal bovine serum without antibiotics. The initial stock cells received from American Type Culture Collection were expanded for cryopreservation in liquid nitrogen. For experiments, PC-3 or DU145 cells were thawed and used for experiments from the third passage after thawing to the 20th passage. TRAMP-C2 cells were obtained from Prof. Margot Cleary of our Institute and grown per conditions as detailed by the originators of this cell line (12). To standardize all PGG/drug exposure conditions, cells were bathed in culture medium at a volume to surface area ratio of 0.2 mL/cm^2 (e.g., 15 mL for a T75 flask and 5 mL for a T25 flask). For the experiments in which caspase inhibitor was used, the inhibitor and PGG were given to the cells at the same time. Dimethylsulfoxide (DMSO; ≤2 μL/mL) was added as a vehicle solvent to the control culture that did not receive the inhibitor. This concentration of DMSO did not cause any adverse morphologic response.

For evaluation of clonogenic ability of PC-3 cells after 3 d of treatment with PGG, the DMSO-exposed and PGG-treated cells (adherent) were trypsinized off the T25 flasks and counted. The cells were diluted and seeded into six-well plates at either 1,000 or 100 cells per well in fresh complete medium. After 11 d of growth, the plates were rinsed with PBS, and the cell colonies were fixed and stained by crystal violet and photographed.

Crystal Violet Staining

For the evaluation of overall inhibitory effect of PGG on cell number, the cells were treated with PGG daily for 4 d. After treatment, the culture medium was removed, and the cells were fixed in 1% glutaraldehyde solution in PBS for 15 min. The fixed cells were stained with 0.02% aqueous solution of crystal violet for 30 min. After washing with PBS, the stained cells were solubilized with 70% ethanol. The absorbance at 570 nm with the reference filter 405 nm was evaluated using a microplate reader (Beckman Coulter, Inc.).

Evaluations of Apoptosis and Other Types of Cell Deaths

Apoptosis was assessed by multiple methods. The first method was immunoblot analysis of cleavage of PARP and/or key procaspases. The second was based on flow cytometric detection of sub-G_1 apoptotic fraction. The third was ELISA detection of oligonucleosomes in apoptotic cells with a kit purchased from Roche Diagnostics Corporation. All these methods were as described previously (13, 14). In addition, we used Annexin V staining of externalized phosphatidylserine to detect early apoptotic cells (propidium iodide excluding, PI–) and later apoptotic/necrotic cells (propidium iodide permeable, PI+) by flow cytometry using a staining kit from MBL International, Inc.

Immunoblot Analyses

The cell lysate was prepared in ice-cold radioimmunoprecipitation assay buffer, as described previously (13). Immunoblot analyses were essentially as described (13), except that the signals were detected by enhanced chemofluorescence with a Storm 840 scanner (Molecular Dynamics).

RNA Interference

The small interfering RNA (siRNA) for human Beclin-1 or death RIP1 was purchased from Santa Cruz Biotechnologies. The cells were transfected with 20 nmol/L siRNAs using INTERFERin transfection reagent (Polyplus-Transfection, Inc.) for 24 h and then were used for subsequent experiments with PGG treatment.

Statistical Analyses

Numerical data were expressed as mean ± SE. Statistical analyses were carried out with Prism and Sigma plot softwares, and $P < 0.05$ was considered statistically significant. The data were analyzed by ANOVA followed by Bonferroni *t* test for pairwise multiple comparisons or other appropriate tests.

Results

PGG Induced Caspase-Independent Programmed Cell Death in PC-3 Prostate Cancer Cells

We have previously reported significant growth inhibitory actions of PGG against DU145 and LNCaP cells through cell cycle G_1 and S arrests and caspase-mediated cell death (5, 15). Here, we examined its potency against another even more aggressive human prostate cancer cell line, PC-3, that is p53 null and known for high AKT activity because of null PTEN status (7) and is highly metastatic when inoculated orthotopically into the prostate of immunodeficient mice. Similar to our earlier report (5), exposure of sparsely seeded PC-3 cells to daily changes of fresh medium (10% fetal bovine serum) containing PGG (50, 75 μmol/L) for 4 days significantly decreased the number of adherent PC-3 cells, with efficacy similar to that against DU145 cells (Fig. 1A).

We have reported recently that PGG induces S and G_1 arrests in not only DU145 and LNCaP cells but also in PC-3 cells (15). The induction of S arrest (through DNA replicative inhibition) occurs at a much lower PGG concentration than that is needed to induce apoptosis. Therefore, the cell cycle arrest actions of PGG probably made a significant contribution to the observed overall growth suppression on PC-3 cells. In addition to cell cycle arrests, we have shown that PGG treatment induced exclusively in DU145 cells caspase-mediated apoptosis in a time- and dose-dependent manner (5). This type of death in DU145 cells was confirmed here by the increased PARP cleavage and increased cleavage activation of caspase-9 (cytochrome *c*/apoptosome intrinsic cascade; refs. 16, 17) and caspase-3 and the disappearance of the full-length pro–caspase-8 due to cleavage (DISC/extrinsic cascade; ref. 16; Fig. 1B, *lane 2* versus *1*). Furthermore, the pan-caspase inhibitor zVADfmk essentially prevented PGG-induced overall cell death estimated by Annexin V staining (PI– and PI+) in this cell line (Fig. 1C, *empty column 4* versus *3*).

However, in PC-3 cells, the same dosage of PGG did not induce detachment of cells in the first 48 hours (not shown) or cause increased PARP cleavage, nor activation of caspase-9 and caspase-3, although pro–caspase-8 was partially processed (Fig. 1B, *lane 4* versus *3*). Consistent with the lack of caspase-9 activation, which requires a functional apoptosome assembled from pro–caspase-9 and cytochrome *c* released from the mitochondria (16, 17), PGG did not cause the loss of mitochondrial transmembrane potential, as measured by the 3,3′-dihexyloxacarbocyanine (6) dye uptake (Supplemental Fig. S1). The PC-3 cells were more resistant to PGG-induced overall death than the DU145 cells (Fig. 1C, *solid column 3* versus *empty column 3*). The pan-caspase inhibitor zVADfmk increased the overall death (Annexin V staining; PI– and PI+) induced by PGG in PC-3 cells (Fig. 1C, *solid column 4* versus *3*, and D, *empty column 4* versus *3*). Using sub-G_1 fraction as an indicator for apoptotic DNA fragmentation, we observed that caspase inhibition blocked this classic type of apoptosis in the PC-3 cells (Fig. 1D, *solid column 4* versus *3*), which represented a rather minor fraction of overall death after 4 days of PGG exposure (Fig. 1D, i.e., compare ~8% sub-G_1 fraction, *solid column 3*, with 48% total dead cells, *empty column 3*).

To determine the generality of the caspase-independent death, we examined the death patterns of TRAMP-C2 cell line derived from a carcinoma of TRAMP mouse (12). The expression of SV40 large T antigen in the TRAMP mouse prostate cells binds and inactivates *p53* and *Rb* tumor suppressor genes to promote cell proliferation. PGG was significantly growth inhibitory on cell number even when assessed at 24 hours of treatment (Fig. 2A), likely due to the much shorter doubling time of these aggressive murine prostate cancer cells. PARP cleavage was observed in the PGG-treated TRAMP-C2 cells with the maximum at

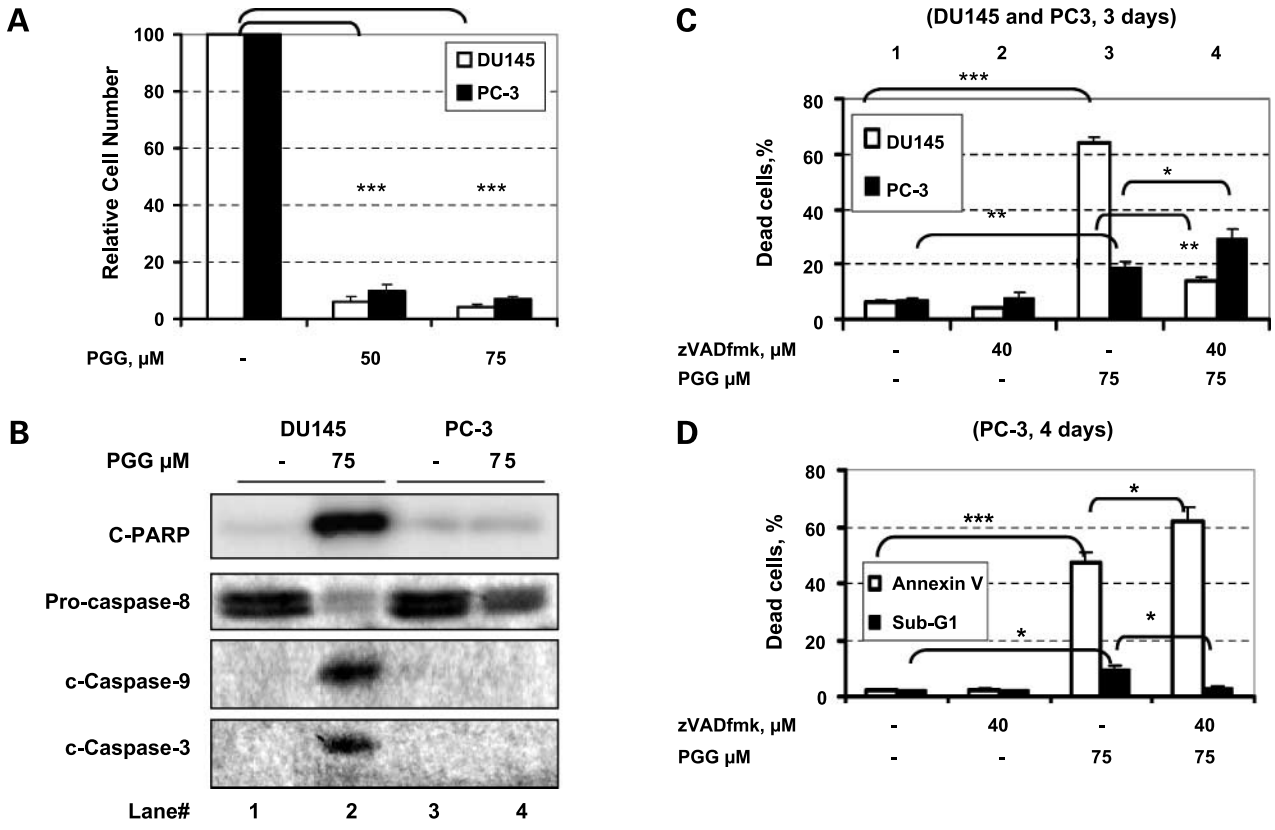

Figure 1. PGG induces caspase-independent death of PC-3 prostate cancer cells. **A,** overall inhibitory effects of PGG on DU145 and PC-3 cell number after 4 d of daily treatment in fresh medium. Expressed as percentage of control cell set as 100. **B,** Western blot analysis of cleavage of PARP and key caspases in DU145 and PC-3 cells after PGG treatment for 48 h. **C,** effects of a pan-caspase inhibitor zVADfmk on PGG-induced death estimated by Annexin V staining (PI− and PI+) in PC-3 (*solid columns*) and DU145 cells (*empty columns*). PGG treatment was for 3 d. **D,** effects of zVADfmk on PGG-induced PC-3 death estimated by Annexin V staining (PI− and PI+; *empty columns*) and apoptosis estimated by sub-G_1 fraction (*solid columns*). PGG treatment was for 4 d. For **A, C,** and **D**, mean ± SE; $n = 3$. *, $P < 0.05$; **, $P < 0.01$; ***, $P < 0.001$.

an intermediate dose of exposure (25 μmol/L). Caspase inhibition in TRAMP-C2 cells did not protect against overall death (total Annexin V staining) induction by PGG (Fig. 2B). These data indicate that, in contrast to DU145 and LNCaP cells in which caspases play crucial mediator roles for their apoptotic death (5), caspases made a minor contribution to the overall cell death in the TRAMP-C2 cell line by PGG as in the PC-3 cells.

Programmed cell deaths, whether apoptotic or not, often require short-lived proteins to mediate the death processes and are attenuated by an inhibition of protein synthesis (for example, refs. 18, 19). Indeed, the protein synthesis inhibitor cycloheximide attenuated the overall death induced by PGG in both TRAMP-C2 and PC-3 cells (Fig. 2C and D). Therefore, whereas PGG induced predominantly zVADfmk-preventable (caspase dependent) apoptosis in DU145 and LNCaP cells (5), the data presented above showed that PGG induced mostly non-zVADfmk-preventable cell death in PC-3 and TRAMP-C2 prostate cancer cells. The protein synthesis inhibitor data supported a programmed nature of the cell death induced by PGG in these cells.

Induction of Autophagic Features by PGG in PC-3 and TRAMP-C2 Cells

Treatment of PC-3 cells with PGG resulted in prominent perinuclear vacuoles that were highly suggestive of autophagy, starting around 2 days of exposure (data not shown). Such changes were not seen in PGG-treated DU145 or LNCaP cells (data not shown). As a biochemical marker for autophagy, the microtubule-associated protein 1 LC3 exists as either an 18-kDa cytosolic protein (LC3-I) and an autophagy-related, C-terminus phosphatidylethanolamine–modified form (LC3-II), which seems as a 16-kDa faster migrating form on SDS-gel (1). PGG treatment of PC-3 cells for 48 and 72 hours upregulated the abundance of LC3-I form and increased the lipid modified LC3-II form at 48 and 72 hours (Fig. 3A). In the TRAMP-C2 cells, we observed also an induction of LC3-II form that was dose-dependent with PGG and was much faster (24 h) than in PC-3 cells (48 hours; Fig. 3A).

To verify the PGG-induced autophagy, we treated stable transfectants of PC-3 cells expressing green fluorescent protein (GFP)–LC3 fusion protein (ref. 20; a generous gift of Prof. S. Singh, University of Pittsburgh) with PGG.

Fluorescence microscopy revealed a diffuse localization of GFP–LC3 in DMSO-treated control cells (Fig. 3B, *DMSO*). In contrast, treatment of cells with PGG for 72 hours produced punctas of GFP–LC3 fluorescence (Fig. 3B, *PGG*). These data together support the induction of autophagosomes by PGG in these prostate cancer cell lines that were less prone to undergo caspase-mediated apoptosis than DU145 or LNCaP cells.

Autophagy Induction by PGG Was Associated with the Inactivation of mTOR–Downstream Targets

Inhibition of the mTOR kinase pathway has been closely associated with autophagy in some models (10). mTOR is a known target of the survival kinase AKT, which inhibits caspase-mediated apoptosis in parts through phosphorylating mitochondrial permeability protein BAD (21), and pro–caspase-9 (22), which is the apical caspase in the intrinsic pathway that can be activated by apoptosome assembled from cytosolic cytochrome *c* released from the mitochondria (16, 17). To determine if PGG-induced autophagy involved these signaling molecules, we examined AKT and mTOR phosphorylation status. As shown in Fig. 3C, PGG treatment for 24 hours modestly increased AKT Ser^{473} phosphorylation and without any effect on the phosphorylation of mTOR on Ser^{2481} and Ser^{2448} in PC-3 cells. Nevertheless, we observed decreased phosphorylation of two mTOR substrates S6K and 4EBP1 in PC-3 cells and TRAMP-C2 cells in a dose-dependent manner (Fig. 3D) and as early as 6 hours of exposure (earliest time point examined) in PC-3 cells (Fig. 3D). These data support an early targeting by PGG of mTOR–downstream effectors, but not mTOR phosphorylations, to induce the subsequent autophagic responses seen at 48 h of PGG exposure and beyond. On the other hand, PGG increased AKT phosphorylation, which could be in part responsible for suppressing the caspase signaling cascades.

mTOR–Inhibitor Rapamycin Attenuated PGG-Induced Death, but an Inhibitor of Autophagy, 3-Methyladenine, Increased Overall Death

Because mTOR inhibition is a classic inducer of autophagy (10), we expect that its inhibitor rapamycin should enhance autophagy induction by PGG in PC-3 cells. We

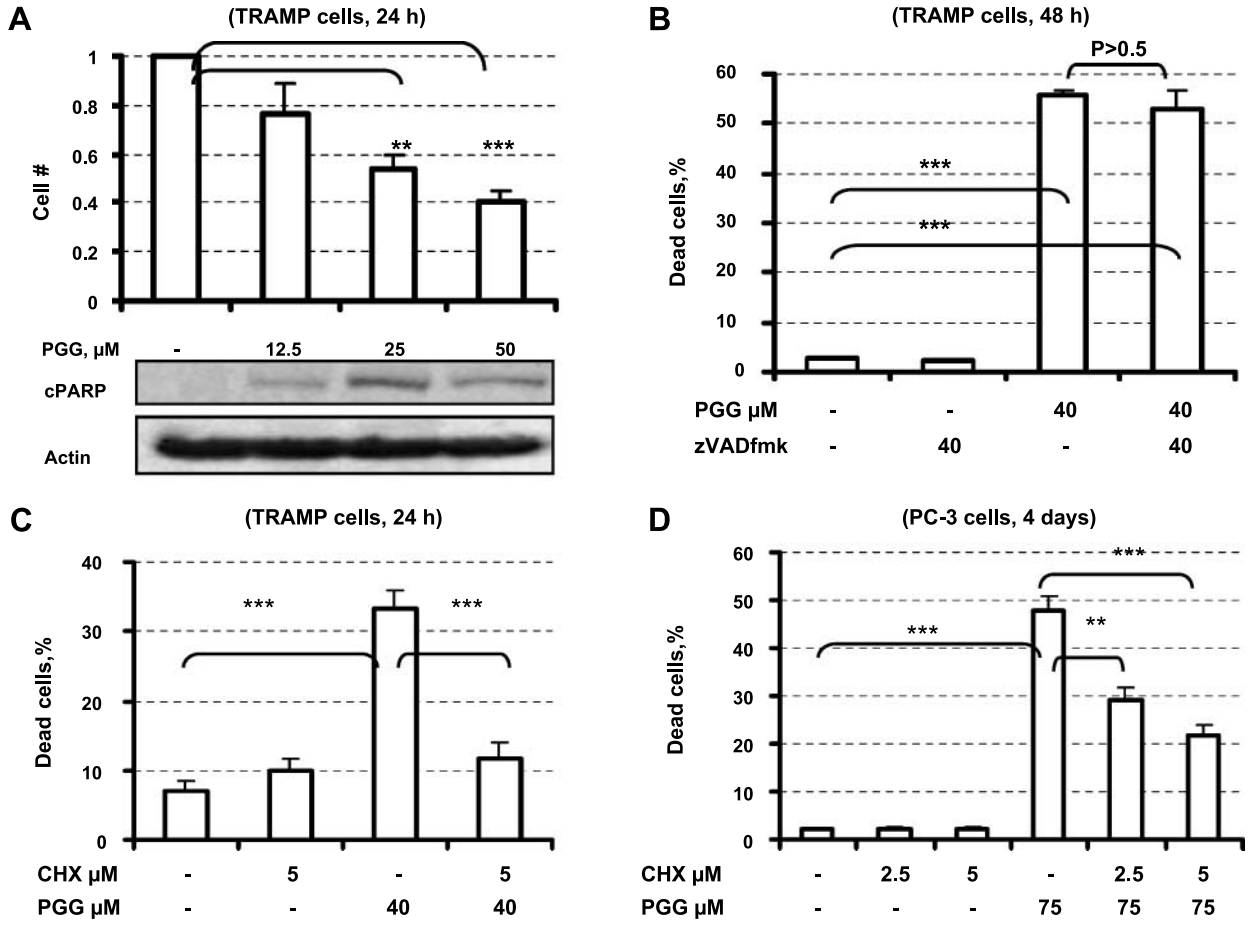

Figure 2. PGG induces predominantly non-zVADfmk-preventable programmed cell death in TRAMP-C2 cells. **A,** effects of PGG on TRAMP cell number after 24 h treatment (*graph*) and PARP cleavage (*immunoblot*). **B,** effects of a pan-caspase inhibitor zVADfmk on PGG-induced death estimated by Annexin V staining (PI− and PI+) in TRAMP-C2 cells. PGG treatment was for 48 h. **C,** effect of protein synthesis inhibitor cycloheximide (CHX) on PGG-induced death estimated by Annexin V staining (PI− and PI+) in TRAMP-C2 cells after 24 h of PGG treatment. **D,** effect of cycloheximide on PGG-induced death estimated by Annexin V staining (PI− and PI+) in PC-3 cells. PGG treatment was for 4 d. Mean ± SE; $n = 3$. **, $P < 0.01$; ***, $P < 0.001$.

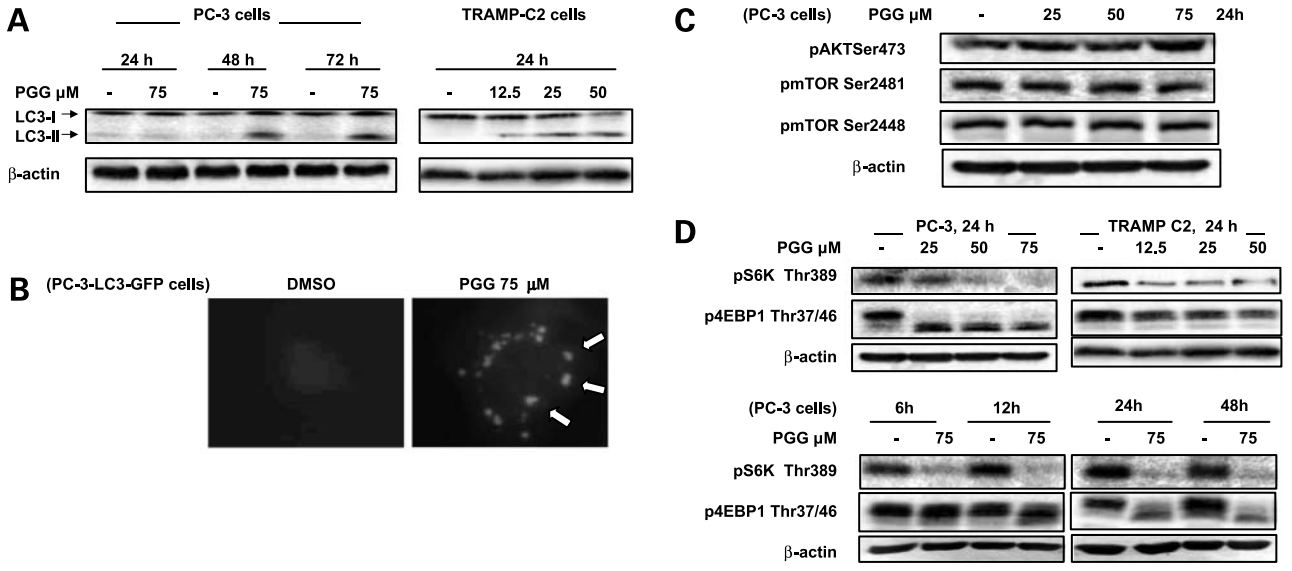

Figure 3. PGG induces autophagic features in PC-3 and TRAMP-C2 cells and dephosphorylation of mammalian target of rapamycin (mTOR) targets S6K and 4EBP1. **A,** Western blot analysis of PGG-induced lipid modification of light chain 3 (LC3) protein in PC-3 and TRAMP-C2 cells. **B,** representative fluorescence microscopy image of stable transfectant PC-3 cells expressing GFP–light chain 3 treated with DMSO vehicle or PGG for 48 h. The intense punctas (some marked by *arrows*) in PGG-treated cells are indicative of autophagosomes. **C,** Western blot analysis of phosphorylation of AKT and mammalian target of rapamycin in PC-3 cells treated with increasing concentrations of PGG for 24 h. **D,** Western blot detection of effects of PGG treatment on the phosphorylation status of S6K and 4EBP1 in PC-3 or TRAMP-C2 cells.

observed that inclusion of rapamycin decreased overall death induced by PGG in PC-3 cells (Annexin V staining PI+ and PI−; Fig. 4A). Western blot analyses showed that rapamycin cotreatment increased PGG-induced LC3-II form but decreased PARP cleavage (Fig. 4A, *blot*).

Conversely, the phosphatidylinositol 3-kinase III–inhibitor 3-methyladenine increased PGG-induced overall cell deaths (Fig. 4B, *column 4* versus *3*). Western blot showed a concordant increase of PARP cleavage. These results together indicated that PGG-induced autophagy protected against overall cell death and caspase-mediated events by PGG in the PC-3 cells.

Beclin-1 Knockdown Enhanced PGG-Induced Apoptosis (Sub-G_1) without Affecting PGG-Induced Cell Cycle Effect

To further test the role of autophagy induction by a genetic approach, we knocked down the autophagy mediator Beclin-1 by siRNA, as confirmed by Western blot (Fig. 4D, *lanes 3* and *5* versus *lanes 1* and *2*). Interestingly, Beclin-1 knockdown did not affect the cell cycle S-arrest by PGG on PC-3 cells (Fig. 4C) but significantly increased (~3-folds) the apoptotic sub-G_1 fraction (Fig. 4C). Western blot for cleaved PARP supported a greatly increased PGG-induced, caspase-mediated apoptosis by knocking down Beclin-1 (Fig. 4D, *lane 5* versus *4*). The enhanced caspase-mediated apoptotic signaling was through increased caspase-9 activation (i.e., mitochondria intrinsic pathway), but not caspase-8 (extrinsic pathway), which was not further affected by Beclin siRNA. Therefore, the presence of functional Beclin-1 and competent autophagy program in PC-3 cells probably played a role in suppressing the mitochondria-apoptosome caspase-9 activation cascades in PGG-treated cells.

Role of Death RIP1 Kinase

Because death RIP1 kinase has been linked to necroptosis, which is a form of cytoplasmic cell death that is associated with autophagy induction when caspases are blocked (2, 3, 23), we knocked down death RIP1 expression by siRNA to determine the effect on PGG-induced overall cell death as well as PARP cleavage (caspase apoptosis) and LC3 modification (autophagy; Fig. 4E). According to Annexin V staining, knocking down death RIP1 increased Annexin V+/PI− (early apoptosis) and the overall death induced by PGG by 2-folds each (*lane 4* versus *2*). However, this did not alter LC3-II level nor did it increase PARP cleavage (Fig. 4E). The data suggested that death RIP1 was involved in suppressing PGG-induced caspase-independent deaths and through pathways independent of autophagy (no change of LC3-II). The data did not support necroptosis in accounting for PGG-induced non-caspase-mediated programmed cell death in PC-3 cells.

Role of Phosphatidylinositol 3-Kinase–AKT in PGG-Induction of Autophagy and Apoptosis

Because we have observed an increased phosphorylation of AKT by PGG in PC-3 (Fig. 3C) and other prostate cancer cell lines such as LNCaP and DU145 (not shown), we interrogated the functional significance of AKT and its upstream kinase phosphatidylinositol 3-kinase in the autophagic response and cell deaths induced by PGG. As shown in Fig. 5A, treatment alone with LY294002, an irreversible phosphatidylinositol 3-kinase inhibitor, in PC-3 cells (high AKT due to null PTEN) did not increase the basal

level of apoptotic death (*column 3* versus *1*) but increased PGG-induced apoptosis, estimated by sub-G_1 fraction (death ELISA for apoptotic nucleosomes showed the same pattern) by more than 3-folds (*column 4* versus *2*). Similarly, LY294002 alone did not increase GFP–LC3 condensation (LC3 punctas) in the PC-3 cells that stably expressed transfected GFP–LC3 without PGG (Fig. 5B, *column 3* versus *1*), but increased this autophagy feature more than 3-folds in PGG-treated cells (Fig. 5B, *column 4* versus *2*). These data suggest that the superactivation of AKT (likely phosphatidylinositol

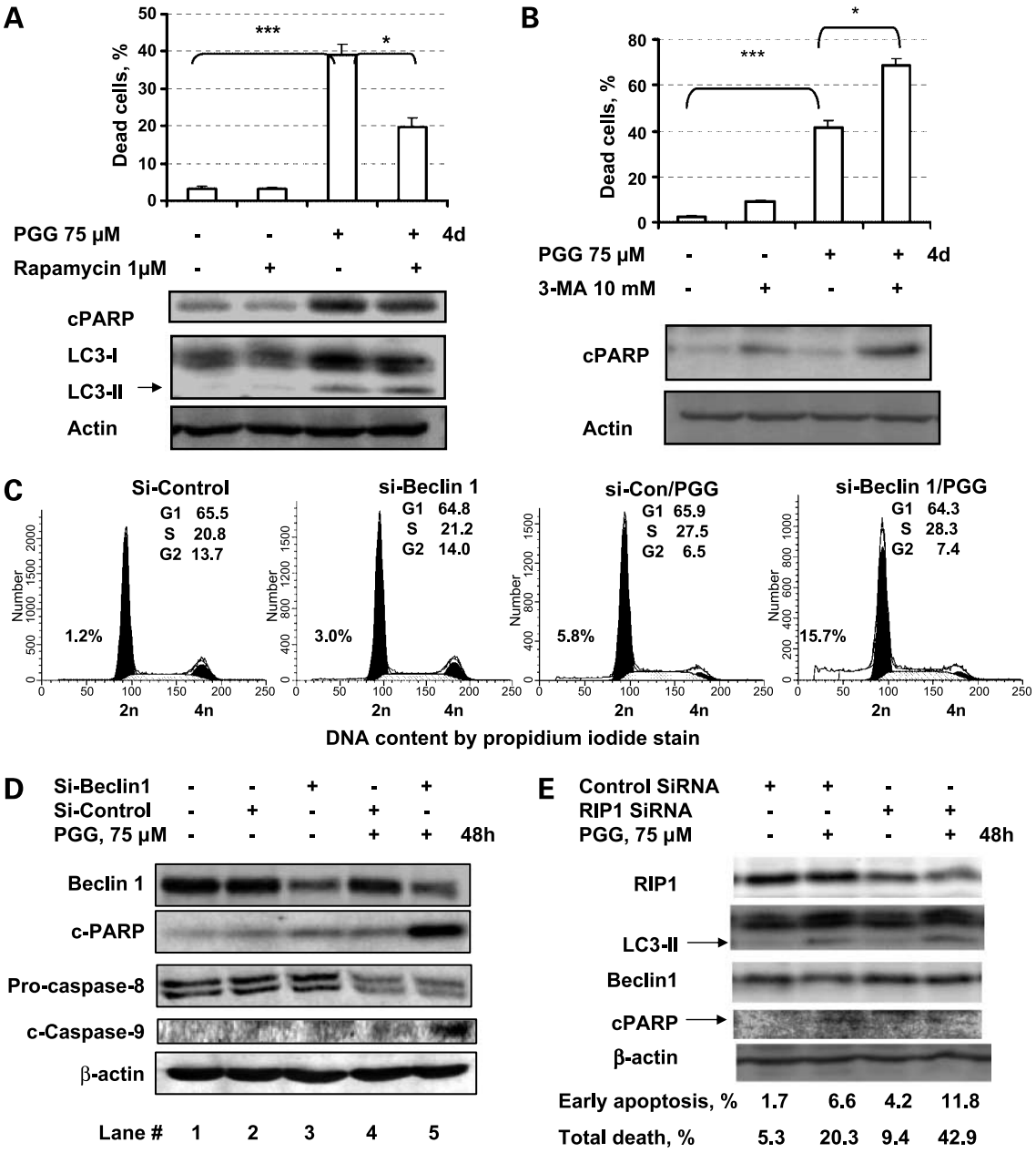

Figure 4. Autophagy induction by PGG inhibits caspase-mediated apoptosis of PC-3 cells. **A,** effect of mammalian target of rapamycin inhibitor rapamycin on PGG-induced death estimated by Annexin V staining (PI− and PI+; *graph*) and PARP cleavage (caspase signaling) and light chain 3 (LC3) lipid modification (autophagy). **B,** effect of autophagy inhibitor 3-methyladenine (3MA) on PGG-induced death estimated by Annexin V staining (PI− and PI+; *graph*) and PARP cleavage (caspase signaling). Mean ± SE; $n = 3$. *, $P < 0.05$; **, $P < 0.01$; ***, $P < 0.001$. **C,** effect of knocking down autophagy-mediating protein Beclin-1 on sub-G_1 apoptotic cell fraction and cell cycle distribution in PC-3 cells. PGG treatment was for 48 h. **D,** Western blot analyses of the effect of knocking down Beclin-1 on PGG-induced caspase-9 cleavage activation and PARP cleavage in PC-3 cells. PGG treatment was for 48 h. **E,** Western blot analyses of the effect of knocking down death receptor-interacting protein 1 (RIP1) on PGG-induced PARP cleavage and light chain 3 modification and cell deaths estimated by Annexin V/PI− (early apoptosis) and Annexin V/PI+ (total death) in PC-3 cells.

3-kinase) by PGG in PC-3 cells attenuated not only apoptosis signaling, as expected, through phosphorylation of BAD (21) and pro–caspase-9 (22) but also the autophagic response.

To further test the specific role of AKT activation, we treated DU145 cells stably transfected with an active AKT (24) with PGG and compared with vector transfectant for cell death. As expected, the AKT-transfectant cells were less sensitive than vector-DU145 cells (low AKT due to wild-type PTEN) to undergo PGG-induced apoptosis (estimated by sub-G_1; Fig. 5C). The pan-caspase inhibitor completely blocked PGG-induced apoptotic sub-G_1 fraction in these AKT-DU145 cells as it did in the vector-DU145 cells (Fig. 5C, *column 4* versus 2). No morphologic features of autophagy were observed after PGG exposure in the AKT-DU145 cells (data not shown). This indicates that restoring AKT in the DU145 cells conferred the known anti-caspase/apoptotic activity against PGG, but these cells did not exhibit an autophagy response with PGG exposure. Examination of Beclin-1 protein level in DU145, LNCaP, or PC-3 cells did not detect any difference among these cell lines (Fig. 5D). Therefore, AKT status or Beclin-1 level in a cell line might not be a determinant of the autophagy signaling by PGG.

PGG Treatment of PC-3 Cells Did Not Induce Reactive Oxygen Species Generation

Because we have shown that reactive oxygen species induction and p53 played a crucial mediating role for caspase-mediated apoptosis by PGG in LNCaP cells (5), we examined PC-3 cells treated with PGG for reactive oxygen species using fluorescence dyes with some specificity for superoxide (hydroethidine) or hydroperoxide (6-carboxy-2′,7′-dichlorodihydrofluorescein diacetate). We did not detect any significant effect of PGG either at 6 or 24 h (Supplemental Fig. S2).

PGG-Treated PC-3 Cells Lost Clonogenic Growth Ability

To determine whether the PGG-treated PC-3 cells lost long-term growth ability, we treated cells with 75 μmol/L

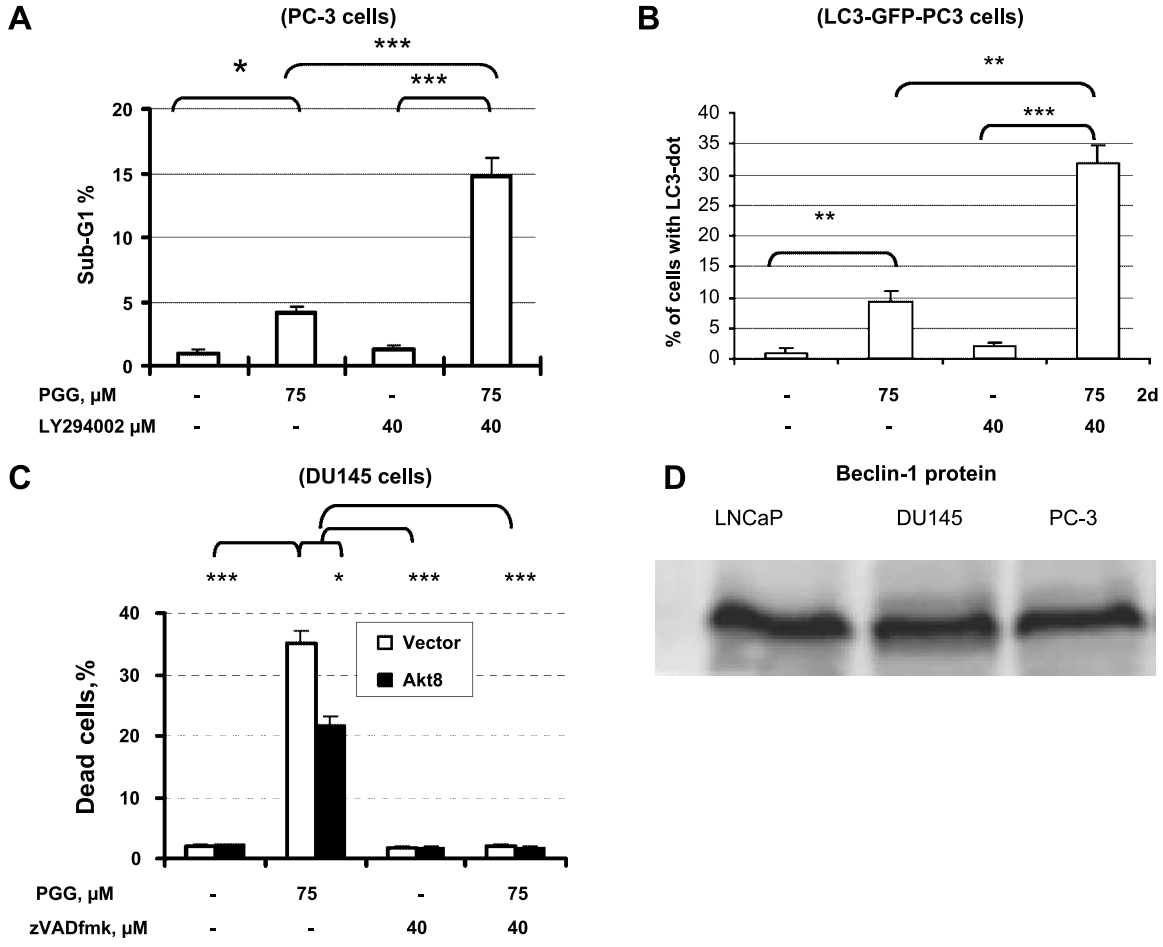

Figure 5. Superactivation of AKT by PGG inhibits caspase-mediated apoptosis. **A,** effect of an irreversible inhibitor of the AKT upstream kinase phosphatidylinositol 3-kinase LY294002 on PGG-induced sub-G_1 apoptotic fraction in PC-3 cells after 48 h PGG treatment. **B,** effect of LY294002 on PGG-induced formation of LC3–GFP punctas (autophagosomes) in LC3–GFP/PC-3 cells after 48 h PGG treatment. **C,** effect of zVADfmk on PGG-induced death (estimated by sub-G_1) of DU145 cells overexpressing a constitutively active AKT (Akt8; ref. 24) after 48 h of PGG treatment. Mean ± SE; $n = 3$. *, $P < 0.05$; **, $P < 0.01$; ***, $P < 0.001$. **D,** Western blot detection of Beclin-1 abundance in PC-3, DU145, and LNCaP cells.

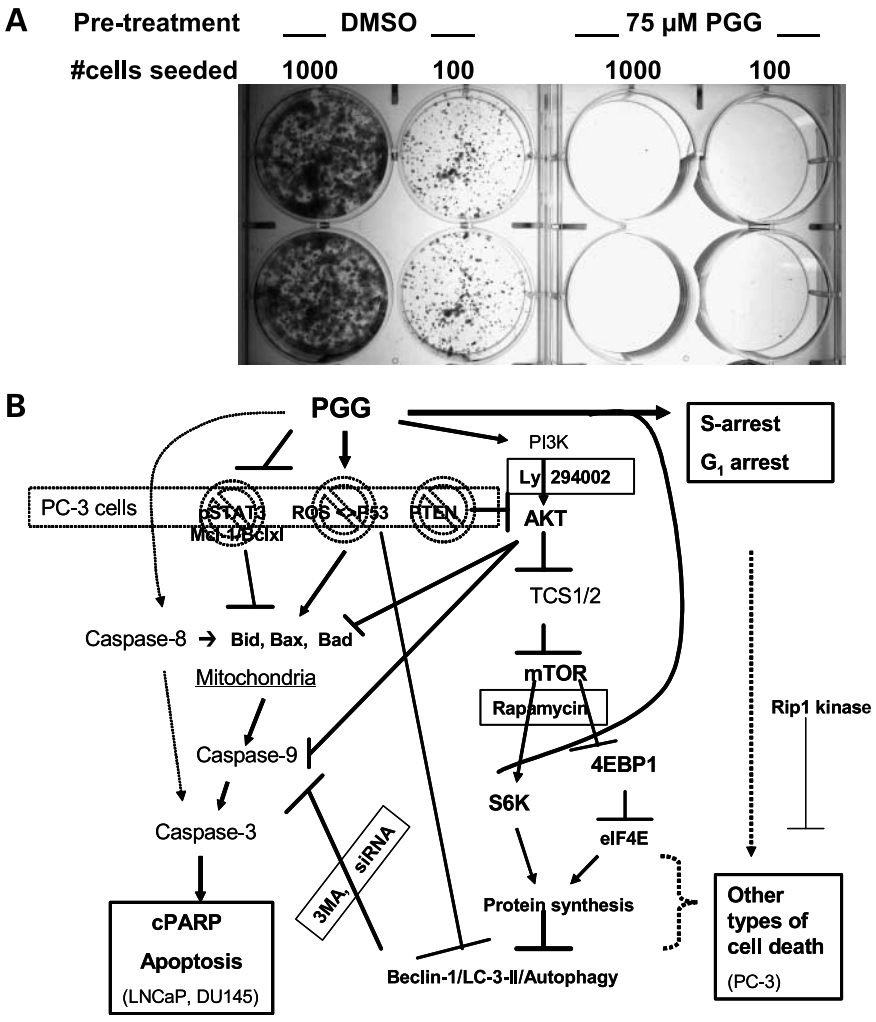

Figure 6. **A,** loss of clonogenic ability after PGG treatment. PC-3 cells were treated with DMSO vehicle or 75 μmol/L PGG for 3 d. The adherent cells were trypsinized off the T25 flasks and seeded at either 1,000 or 100 cells per well in six-well plates in fresh complete medium. After 11 d of growth, the plates were stained by crystal violet and photographed. **B,** possible signaling events in PGG-induced autophagy and programmed deaths of PC-3 cells in reference to events in LNCaP and DU145 cells (5). The nature of the programmed cell death in PC-3 needs further clarification.

PGG for 3 days and then replated the cells sparsely (100 and 1,000 cells per well in six-well plates) in fresh complete medium. When examined 11 days later, the DMSO vehicle–treated cells grew into visible colonies, whereas PGG-treated cells failed to grow at all (Fig. 6A). The data therefore support PGG treatment caused an irreversible loss of clonogenic ability through non-caspase-mediated programmed cell death in the caspase apoptosis–resistant PC-3 cells.

Discussion

The most salient features of the data presented above supported the induction by PGG of caspase-independent programmed cell death accompanied by autophagic features in PC-3 cells and TRAMP-C2 cells (Figs. 1–3) and that PGG-treated PC-3 cells for 3 days completely lost the clonogenic potential (Fig. 6A), supporting the irreversible nature of the programmed cell death. To our knowledge, this is the first such report of autophagy responses induced by PGG, an anticancer herbal compound with known *in vivo* efficacy against cancers of a number of organ sites, including prostate (5, 6), lung (11), and breast.[4] These findings might be especially meaningful in light of the recently reported *in vivo* efficacy of PGG against the growth of PC-3 cells inoculated intratibially in the athymic nude mice (6).

Compared with DU145 (Fig. 1B) and LNCaP cells (5), there was a clear suppression of PGG-induced, caspase-mediated apoptosis execution in the PC-3 cells (Fig. 1B), despite the processing of pro–caspase-8 (Fig. 1B). The lack of caspase-9 cleavage (Fig. 1B) and preservation of mitochondrial transmembrane potential/integrity in PGG-treated PC-3 cells (Supplementary Fig. S1) suggest the lack of formation of PGG-induced functional apoptosomes to efficiently process the intrinsic caspase cascades in PC-3 cells. The high AKT in PC-3 cells due to null PTEN plus its superactivation by PGG (Fig. 3C) could be one mechanism for the suppression of mitochondria driven apoptosome activation of the caspase-9 cascade of apoptosis execution in these cells. The role of AKT to suppress mitochondria/caspase-9

[4] Lee et al., unpublished observation.

cascade is well established through the phosphorylation of the mitochondrial permeability protein BAD (21) and that of pro–caspase-9 itself to prevent its activation (22). Because of high AKT, PC-3 and LNCaP cells are also resistant to apoptosis induction by the death receptor ligand TRAIL through the extrinsic route (DR4/DR5 forming DISC to cleave and activate pro–caspase-8), in part because of failure of cross-talk to the mitochondria/caspase-9 cascade, which amplifies the overall death execution (25–27). This speculation was supported by the increased caspase-mediated apoptosis by combining PGG with phosphatidylinositol 3-kinase–AKT inhibition (Fig. 5A) or decreased death by ectopic expression of the active AKT in DU145 cells (Fig. 5C).

In addition to the high basal AKT, PC-3 cells lack p53, which transcriptionally regulates mitochondria permeability-targeting Bcl-2 family protein BAX (28) and p53-upregulated mediator of apoptosis (PUMA; refs. 29, 30), which affect mitochondria integrity and intrinsic death signaling, as well as the death receptors DR4/DR5 (31, 32), which engage caspase-8 signaling through the extrinsic pathway. More recently, studies have identified the direct action of cytosolic/mitochondrial p53 through binding to Bax to effect mitochondria outer membrane permeability (33). A tripartite nexus between antiapoptotic Bcl-xL protein, cytoplasmic p53, and PUMA coordinates the cytosolic versus nuclear p53 death functions. After genotoxic stress, Bcl-xL sequesters cytoplasmic p53. Nuclear p53 causes the expression of PUMA, which then displaces p53 from Bcl-xL, allowing p53 to induce mitochondrial permeabilization (34). p53 has been linked to amplification of reactive oxygen species generation from the mitochondria after caspase-mediated cleavages (35, 36). Because we have shown that p53 plays a crucial role in mediating caspase-mediated apoptosis in LNCaP cells (5), the lack of p53 in PC-3 cells probably also played a crucial role for the failure of PGG to induce reactive oxygen species (Supplementary Fig. S2) and mitochondrial permeability loss (Supplementary Fig. S1) and caspase-9–mediated apoptosis (Fig. 1B). Furthermore, PC-3 cells lack constitutively activated STAT3, which regulates the transcription of mitochondrial protective Bcl-2 related proteins such as Mcl-1 and Bcl-xL. This feature, in contrast to DU145 cells (5), might remove yet another pathway for PGG to signal to mitochondria/caspase-9 cascade. Figure 6B summarized these major cell death signaling and execution events affected by PGG based on data presented here in PC-3 cells and our published data in DU145 and LNCaP cells (5).

Our research focused on generating data to address questions about the functional significance of the autophagy responses, the possible signaling mechanisms, and what regulate/determine cell death fates. In terms of functional significance, mechanistic investigations showed that the autophagic responses induced by PGG in PC-3 cells provided survival signaling that suppressed caspase-mediated and apoptotic deaths, as shown with a pharmacologic inducer, rapamycin (Fig. 4A), and an inhibitor of autophagy, 3-methyladenine (Fig. 4B), or by knocking down an autophagy mediator molecule, Beclin-1 (Fig. 4C and D). As for molecular events associated with autophagy induction/signaling, the observed rapid inhibition of the phosphorylation of mTOR–downstream targets S6K and 4EBP1 by PGG in PC-3 and TRAMP-C2 cells (Fig. 3C and D) suggest that PGG targeted signaling downstream of rather than the mTOR itself. The rapidity of such signaling changes at least 24 hours ahead of the onset of autophagy (LC3-II) and programmed cell death in PC-3 cells (Fig. 3A) supports them as primary events in autophagy induction.

Although AKT levels differed vastly among the three human prostate cancer cell lines (24), our data did not support AKT level as a key determinant of autophagy induction by PGG (Fig. 5). It is interesting that PGG increased AKT phosphorylation, a feature that resembled rapamycin in that rapamycin binds and inhibits mTOR enzymatic activity but through a feedback loop upregulates AKT expression and activity (37–39). Because PGG did not affect mTOR phosphorylation status, whether it directly inhibits mTOR enzymatic activity or interferes with mTOR complex formation with Raptor should be investigated.

Wild-type p53 and certain cytoplasmic p53 mutants have recently been shown to suppress autophagy (40–42). Consistent with this, we found that, in LNCaP cells, attenuation of p53 by siRNA decreased PGG-induced caspase-mediated cPARP cleavage as expected (5) and increased autophagic marker light chain II after 3 days of treatment (Supplementary Fig. S3). Whether the void of functional p53 in PC-3 cells plays a determinant role for autophagy signaling by PGG in these cells requires further investigation.

However, the exact nature of the programmed cell death, other than autophagy and caspase-mediated apoptosis, after prolonged exposure to PGG remains unclear and requires further investigation. Because death receptor-interacting protein 1 knockdown did not protect the cells and, instead, this manipulation increased overall death (Fig. 4E), it is not likely that necroptosis was the mediating noncaspase programmed cell death. The data did not support death RIP1 as a mediator of PGG induction of autophagy either, in contrast to its key role in other well-established models of autophagy (23).

In summary, the significant growth suppression activity of PGG (Fig. 1A) and a complete loss of clonogenic potential of PGG-treated PC-3 cells (Fig. 6A), through a possible induction of caspase-independent programmed cell death, as well as its potent induction of cell cycle arrests (G_1 and S; ref. 25), provided potential mechanisms to account for the observed *in vivo* efficacy of PGG against the growth of PC-3 cells inoculated intratibially (6). The results support further investigation of its merit as a potential drug candidate for therapy of caspase-resistant recurrent prostate cancer, either as a single modality or in combination with other drugs.

Disclosure of Potential Conflicts of Interest

No potential conflicts of interest were disclosed.

Acknowledgments

We thank Professor S. Singh, University of Pittsburgh, for the PC-3 cells stably transfected with GFP–light chain 3; and Todd Schuster, Hormel Institute Shared Instruments Facility, for doing flow cytometry and Annexin V staining.

References

1. Kroemer G, Galluzzi L, Vandenabeele P, et al. Classification of cell death: recommendations of the Nomenclature Committee on Cell Death 2009. Cell Death Differ 2009;16:3–11.

2. Festjens N, Vanden Berghe T, Cornelis S, Vandenabeele P. RIP1, a kinase on the crossroads of a cell's decision to live or die. Cell Death Differ 2007;14:400–10.

3. Vandenabeele P, Vanden Berghe T, Festjens N. Caspase inhibitors promote alternative cell death pathways. Sci STKE 2006;2006:e44.

4. Kroemer G, Jaattela M. Lysosomes and autophagy in cell death control. Nat Rev Cancer 2005;5:886–97.

5. Hu H, Lee HJ, Jiang C, et al. Penta-1,2,3,4,6-O-galloyl-β-D-glucose induces p53 and inhibits STAT3 in prostate cancer cells *in vitro* and suppresses prostate xenograft tumor growth *in vivo*. Mol Cancer Ther 2008;7:2681–91.

6. Kuo PT, Lin TP, Liu LC, et al. Penta-O-galloyl-β-D-glucose suppresses prostate cancer bone metastasis by transcriptionally repressing EGF-induced MMP-9 expression. J Agric Food Chem 2009;57:3331–9.

7. van Bokhoven A, Varella-Garcia M, Korch C, et al. Molecular characterization of human prostate carcinoma cell lines. Prostate 2003;57:205–25.

8. Shin DS, Kim HN, Shin KD, et al. Cryptotanshinone inhibits constitutive signal transducer and activator of transcription 3 function through blocking the dimerization in DU145 prostate cancer cells. Cancer Res 2009;69:193–202.

9. Levine B, Sinha S, Kroemer G. Bcl-2 family members: dual regulators of apoptosis and autophagy. Autophagy 2008;4:600–6.

10. Guertin DA, Sabatini DM. An expanding role for mTOR in cancer. Trends Mol Med 2005;11:353–61.

11. Huh JE, Lee EO, Kim MS, et al. Penta-O-galloyl-β-D-glucose suppresses tumor growth via inhibition of angiogenesis and stimulation of apoptosis: roles of cyclooxygenase-2 and mitogen-activated protein kinase pathways. Carcinogenesis 2005;26:1436–45.

12. Foster BA, Gingrich JR, Kwon ED, Madias C, Greenberg NM. Characterization of prostatic epithelial cell lines derived from transgenic adenocarcinoma of the mouse prostate (TRAMP) model. Cancer Res 1997;57:3325–30.

13. Jiang C, Wang Z, Ganther H, Lu J. Caspases as key executors of methyl selenium-induced apoptosis (anoikis) of DU-145 prostate cancer cells. Cancer Res 2001;61:3062–70.

14. Hu H, Jiang C, Ip C, Rustum YM, Lu J. Methylseleninic acid potentiates apoptosis induced by chemotherapeutic drugs in androgen-independent prostate cancer cells. Clin Cancer Res 2005;11:2379–88.

15. Hu H, Zhang J, Lee HJ, Kim SH, Lu J. Penta-O-galloyl-β-D-glucose induces S- and G(1)-cell cycle arrests in prostate cancer cells targeting DNA replication and cyclin D1. Carcinogenesis 2009;30:818–23.

16. Budihardjo I, Oliver H, Lutter M, Luo X, Wang X. Biochemical pathways of caspase activation during apoptosis. Annu Rev Cell Dev Biol 1999;15:269–90.

17. Jiang X, Wang X. Cytochrome *c*-mediated apoptosis. Annu Rev Biochem 2004;73:87–106.

18. Ruchaud S, Seite P, Foulkes NS, Sassone-Corsi P, Lanotte M. The transcriptional repressor ICER and cAMP-induced programmed cell death. Oncogene 1997;15:827–36.

19. Vento R, Giuliano M, Lauricella M, Carabillo M, Di Liberto D, Tesoriere G. Induction of programmed cell death in human retinoblastoma Y79 cells by C2-ceramide. Mol Cell Biochem 1998;185:7–15.

20. Herman-Antosiewicz A, Johnson DE, Singh SV. Sulforaphane causes autophagy to inhibit release of cytochrome *c* and apoptosis in human prostate cancer cells. Cancer Res 2006;66:5828–35.

21. del Peso L, Gonzalez-Garcia M, Page C, Herrera R, Nunez G. Interleukin-3-induced phosphorylation of BAD through the protein kinase Akt. Science 1997;278:687–9.

22. Cardone MH, Roy N, Stennicke HR, et al. Regulation of cell death protease caspase-9 by phosphorylation. Science 1998;282:1318–21.

23. Degterev A, Hitomi J, Germscheid M, et al. Identification of RIP1 kinase as a specific cellular target of necrostatins. Nat Chem Biol 2008;4:313–21.

24. Hu H, Jiang C, Li G, Lu J. PKB/AKT and ERK regulation of caspase-mediated apoptosis by methylseleninic acid in LNCaP prostate cancer cells. Carcinogenesis 2005;26:1374–81.

25. Nesterov A, Lu X, Johnson M, Miller GJ, Ivashchenko Y, Kraft AS. Elevated AKT activity protects the prostate cancer cell line LNCaP from TRAIL-induced apoptosis. J Biol Chem 2001;276:10767–74.

26. Rokhlin OW, Guseva N, Tagiyev A, Knudson CM, Cohen MB. Bcl-2 oncoprotein protects the human prostatic carcinoma cell line PC3 from TRAIL-mediated apoptosis. Oncogene 2001;20:2836–43.

27. Hu H, Jiang C, Schuster T, Li GX, Daniel PT, Lu J. Inorganic selenium sensitizes prostate cancer cells to TRAIL-induced apoptosis through superoxide/p53/Bax-mediated activation of mitochondrial pathway. Mol Cancer Ther 2006;5:1873–82.

28. Miyashita T, Reed JC. Tumor suppressor p53 is a direct transcriptional activator of the human *bax* gene. Cell 1995;80:293–9.

29. Nakano K, Vousden KH. *PUMA*, a novel proapoptotic gene, is induced by p53. Mol Cell 2001;7:683–94.

30. Yu J, Zhang L, Hwang PM, Kinzler KW, Vogelstein B. PUMA induces the rapid apoptosis of colorectal cancer cells. Mol Cell 2001;7:673–82.

31. Liu X, Yue P, Khuri FR, Sun SY. p53 Upregulates death receptor 4 expression through an intronic p53 binding site. Cancer Res 2004;64:5078–83.

32. Sheikh MS, Burns TF, Huang Y, et al. p53-Dependent and -independent regulation of the death receptor *KILLER/DR5* gene expression in response to genotoxic stress and tumor necrosis factor α. Cancer Res 1998;58:1593–8.

33. Chipuk JE, Kuwana T, Bouchier-Hayes L, et al. Direct activation of Bax by p53 mediates mitochondrial membrane permeabilization and apoptosis. Science 2004;303:1010–4.

34. Chipuk JE, Bouchier-Hayes L, Kuwana T, Newmeyer DD, Green DR. PUMA couples the nuclear and cytoplasmic proapoptotic function of p53. Science 2005;309:1732–5.

35. Sayan BS, Sayan AE, Knight RA, Melino G, Cohen GM. p53 Is cleaved by caspases generating fragments localizing to mitochondria. J Biol Chem 2006;281:13566–73.

36. Liu B, Chen Y, St Clair DK. ROS and p53: a versatile partnership. Free Radic Biol Med 2008;44:1529–35.

37. Wan X, Harkavy B, Shen N, Grohar P, Helman LJ. Rapamycin induces feedback activation of Akt signaling through an IGF-1R-dependent mechanism. Oncogene 2007;26:1932–40.

38. O'Reilly KE, Rojo F, She QB, et al. mTOR inhibition induces upstream receptor tyrosine kinase signaling and activates Akt. Cancer Res 2006;66:1500–8.

39. Sun SY, Rosenberg LM, Wang X, et al. Activation of Akt and eIF4E survival pathways by rapamycin-mediated mammalian target of rapamycin inhibition. Cancer Res 2005;65:7052–8.

40. Tasdemir E, Maiuri MC, Galluzzi L, et al. Regulation of autophagy by cytoplasmic p53. Nat Cell Biol 2008;10:676–87.

41. Tasdemir E, Maiuri MC, Orhon I, et al. p53 Represses autophagy in a cell cycle-dependent fashion. Cell Cycle 2008;7:3006–11.

42. Morselli E, Tasdemir E, Maiuri MC, et al. Mutant p53 protein localized in the cytoplasm inhibits autophagy. Cell Cycle 2008;7:3056–61.